

Harmful algae bloom monitoring via a sustainable, sail-powered mobile platform for in-land and coastal monitoring

Jordon S. Beckler^{1*}, Ethan Arutunian², Robert D. Currier³, Eric Milbrandt⁴, Scott Duncan²

¹Harbor Branch Oceanographic Institute, Florida Atlantic University, United States, ²Navocean, United States, ³Gulf of Mexico Coastal Ocean Observing System Regional Association, United States, ⁴Sanibel Captiva Conservation Foundation, United States

Submitted to Journal:
Frontiers in Marine Science

Specialty Section:
Ocean Observation

Article type:
Technology Report Article

Manuscript ID:
437032

Received on:
15 Nov 2018

Frontiers website link:
www.frontiersin.org

In review

Conflict of interest statement

The authors declare that the research was conducted in the absence of any commercial or financial relationships that could be construed as a potential conflict of interest

Author contribution statement

JB authored the manuscript, provided scientific oversight, and participated in field campaigns, EA is the lead designer of the autonomous vehicle hardware and software, RC developed live data visualization interface, EM coordinated field campaigns, and SD designed the sailboat and conducted deployments.

Keywords

Autonomous & remotely-operated vehicle, harmful algal bloom, Mapping, *Karenia brevis* HABs, CDOM, Ocean observation, West Florida Shelf, surface vehicle

Abstract

Word count: 222

Harmful algae blooms (HAB) in coastal marine environments are increasing in number and duration, pressuring local resource managers to implement mitigation solutions to protect human and ecosystem health. However, insufficient spatial and temporal observations create uninformed management decisions. In order to better detect and map blooms, as well as the environmental conditions responsible for their formation, long-term, unattended observation platforms are desired. In this article, we describe a new cost-efficient, autonomous, mobile platform capable of accepting several sensors that can be used to monitor harmful algae blooms in near real-time. The Navocean autonomous sail-powered surface vehicle is deployable by a single person from shore, capable of waypoint navigation in shallow and deep waters, and powered completely by renewable energy. We present results from three surveys of the Florida Red Tide harmful algae bloom (*Karenia brevis*) of 2017-2018. The vessel made significant progress towards waypoints regardless of wind conditions while underway chl. a measurements revealed HAB bloom patches and CDOM and turbidity provided environmental contextual information. While the autonomous sailboat directly adds to our HAB monitoring capabilities, the boat can also help to ground-truth and thus improve satellite monitoring of HABs. Finally, several other pending and future use cases for coastal and inland monitoring are discussed. To our knowledge, this is the first demonstration of a sail-driven vessel used for coastal HAB monitoring.

Funding statement

This work was supported in part by a National Academies Gulf Research Program Early Career Fellowship award #2000007281 that supporting salary and supplies, and the Gulf of Mexico Coastal Ocean Observation System #NA16NOS0120018 that supported salaries.

Ethics statements

(Authors are required to state the ethical considerations of their study in the manuscript, including for cases where the study was exempt from ethical approval procedures)

Does the study presented in the manuscript involve human or animal subjects: No

Data availability statement

Generated Statement: All datasets generated for this study are included in the manuscript and the supplementary files.

Harmful algae bloom monitoring via a sustainable, sail-powered mobile platform for in-land and coastal monitoring

1 **Jordon S. Beckler^{1*,‡}, Ethan Arutunian², Bob Currier³, Eric Milbrandt⁴, Scott Duncan²**

2 ¹Geochemical Sensing Laboratory, FAU Harbor Branch Oceanographic Institute, Ft. Pierce, Florida,
3 USA

4 ²Navocean Inc., Seattle, Washington, USA

5 ³Gulf of Mexico Coastal Ocean Observation System (GCOOS), Texas A&M University, College
6 Station, Texas, USA

7 ⁴SCCF Marine Laboratory, Sanibel Captiva Conservation Foundation, Sanibel, Florida, USA

8

9 *** Correspondence:**

10 Corresponding Author

11 jbeckler@fau.edu

12 **‡Formerly:**

13 Ocean Technology Research Program, Mote Marine Laboratory, Sarasota, Florida, USA

14 **Keywords: Autonomous & Remotely Operated Vehicle¹, Harmful Algal Bloom², Mapping³,**
15 ***Karenia brevis* HABs⁴, CDOM⁵, Turbidity⁶, West Florida Shelf⁷, Surface Vehicle⁸**

16 **Abstract**

17 Harmful algae blooms (HAB) in coastal marine environments are increasing in number and duration,
18 pressuring local resource managers to implement mitigation solutions to protect human and
19 ecosystem health. However, insufficient spatial and temporal observations create uninformed
20 management decisions. In order to better detect and map blooms, as well as the environmental
21 conditions responsible for their formation, long-term, unattended observation platforms are desired.
22 In this article, we describe a new cost-efficient, autonomous, mobile platform capable of accepting
23 several sensors that can be used to monitor harmful algae blooms in near real-time. The Navocean
24 autonomous sail-powered surface vehicle is deployable by a single person from shore, capable of
25 waypoint navigation in shallow and deep waters, and powered completely by renewable energy. We
26 present results from three surveys of the Florida Red Tide harmful algae bloom (*Karenia brevis*) of
27 2017-2018. The vessel made significant progress towards waypoints regardless of wind conditions
28 while underway chl. *a* measurements revealed HAB bloom patches and CDOM and turbidity
29 provided environmental contextual information. While the autonomous sailboat directly adds to our
30 HAB monitoring capabilities, the boat can also help to ground-truth and thus improve satellite
31 monitoring of HABs. Finally, several other pending and future use cases for coastal and inland
32 monitoring are discussed. To our knowledge, this is the first demonstration of a sail-driven vessel
33 used for coastal HAB monitoring.

34 1 Introduction

35 In the last few decades, harmful algae blooms (HABs) have increased in number, intensity, and
36 duration due to cultural eutrophication, increasing rainfall, and warming temperatures (Brand and
37 Compton, 2007; O’Neil et al., 2012). Through the generation of toxins or by creating locally hypoxic
38 conditions, HAB effects can range from acute sickness and respiratory irritation potentially affecting
39 local economies (Backer et al., 2010; Hoagland et al., 2009; Kirkpatrick et al., 2006), to massive
40 marine fish and mammal mortality events (Gannon et al., 2009; Scholin et al., 2000), or even to
41 chronic human poisoning and death through ingestion of contaminated shellfish or drinking water
42 (Carmichael, 2001; Fleming et al., 2002; Reich et al., 2015). HAB blooms are most frequently
43 observed and anthropogenically detrimental in coastal or in-land marine and freshwater bodies
44 (Anderson et al., 2002), for example in areas with coastal recreation, fishing, mari/aquaculture, and
45 drinking water intake systems. Recent years have experienced superlative HAB events with
46 unparalleled public recognition, for example the summer of 2014 and 2016 *Microcystis aeruginosa*
47 blue-green cyanoblooms in Lake Erie and the Indian River Lagoon (Florida) (Smith et al., 2015;
48 Stockley et al., 2018) that poisoned drinking water and decreased property values, respectively, the
49 *Pseudo-nitzschia* bloom of 2015 in California waters that led to the closing of the dungeoness crab
50 fishing season (McCabe et al., 2016), and the 2017-2018 *Karenia brevis* bloom in west Florida
51 (ongoing as of the time of writing) that has led to a declaration of a state of emergency. This “Florida
52 Red Tide” bloom is poised to be the worst on record and has brought an unprecedented amount of
53 national attention to this particular HAB (Ducharme, 2018).

54 To plan for and mitigate the occurrence and effects of HABs, it is ideal to both monitor the algae
55 and/or toxins directly and collect additional ancillary information regarding the chemical and
56 physical ecology of the ecosystems. Traditional routine monitoring is inherently expensive, time
57 consuming, and the spatial and temporal resolution of discrete measurements in many HAB-prone
58 regions is often not sufficient to elucidate bloom causes or properly initiate models. According to a
59 recent HAB scientist community consensus, an observing system consisting of satellite, moored, and
60 mobile data collection platforms will most likely emerge as the most effective holistic approach
61 (Bowers and Smith, 2017). Careful consideration must be given to important tradeoffs existing
62 between sensor specificity targets (e.g. pigments, species, or toxins) and platform compatibility (i.e.
63 fixed location versus mobile), which together determine cost, sampling resolution, and reliability. For
64 example, while satellite-based remote sensing is inexpensive, the technique suffers from insufficient
65 temporal (e.g. daily) and spatial resolution (e.g. ~ 1km), non-species specificity, and interferences
66 from the seafloor, suspended sediment, and clouds. Fixed-location, unattended monitoring devices
67 (i.e. shoreline or moorings) have drastically advanced the temporal resolution of data collection,
68 especially at the species level (Smith et al., 2015; Stockley et al., 2018), but the installation of enough
69 locations to provide sufficient spatial resolution is cost-prohibitive (Shapiro et al., 2015). Given the
70 vertical heterogeneity of HABs, 3-dimensional monitoring platforms, such ocean-going autonomous
71 underwater vehicle buoyancy gliders, are promising and have been successfully deployed in near-
72 shore and open ocean environments (Robbins et al., 2006). However, the submerged nature of these
73 vehicles creates communications, power, and reliability constraints that currently limit sensor options
74 and few species-level options exist. In turn, 2-dimensional Autonomous Surface Vehicles (ASV)
75 such as those powered by sail or waves e.g. “Wave Gliders” or Sairdrone (Daniel et al., 2011; Mordy
76 et al., 2017) may alleviate these constraints and are arguably more favorable for more complex
77 instrumentation. However, to our knowledge, all existing long-duration autonomous vehicles are not
78 designed to operate effectively in shallow and/or near-shore waters less than a few meters depth, their
79 size, form or performance prohibit shallow water operation, and their operation is challenging for
80 non-expert resource managers.

81 For over a decade on the southwest Florida Shelf, fixed location, species-specific optical devices (i.e.
82 Optical Phytoplankton Discriminators; OPD) have been employed as part of a State of Florida and
83 NOAA funded HAB observatory (Sarasota Operations of the Coastal Ocean Observing Lab of Mote
84 Marine Laboratory; SO-COOL). Additionally, AUVs (Slocum gliders) outfitted with either an OPD
85 or a chl. *a* fluorometer are also routinely used to locate and track *K. brevis* HABs (Shapiro et al.,
86 2015). While these efforts have yielded valuable insights into the conditions surrounding HAB bloom
87 formation, these glider operations have presented challenges over the years. Deployments are
88 logistically challenging, requiring an initial transit to deeper waters, and once deployed, a minimum
89 depth limitation of 10 meters (i.e. 20 km from the coast). Finally, cost has prohibited sufficient
90 spatial and temporal coverage, and deployments have been met with unanticipated buoyancy-related
91 operational challenges such as aborts due to nuisance “suckerfish” attaching and sinking gliders (i.e.
92 remora fish).

93 In 2016, Mote Marine Laboratory began a collaboration with Navocean, Inc., to utilize their
94 autonomous sail-powered surface vehicle for *K. brevis* bloom monitoring. Navocean offers small, 2-
95 m in length vessels that are reliable, and can accept versatile sensors. Navocean boats fill a current
96 niche in both the Autonomous Surface Vehicle (ASV) and the HAB mapping markets, being
97 powered solely from renewable sources, inexpensive, navigable in shallow waters (> 1 m), and
98 deployable from shore by a single person. To demonstrate proof of concept for HAB monitoring, a
99 Navocean *Nav2* boat was outfitted with a 3-channel fluorometer (Turner Designs) configured to
100 measure chl. *a* as a proxy for phytoplankton pigments, as well as CDOM and turbidity to provide
101 ancillary environmental information. The boat was deployed for periods of up to one week in the
102 Winter of 2017, during the start of what has become one of the worst *K. brevis* blooms on record.
103 This work describes the system design, testing, and in situ validation, then discusses other potential
104 applications for HAB monitoring and other environmental applications for this unique vehicle.

105 2 Vessel Design and Operation

106 The *Nav2* ASV (**Figure 1**) is small, lightweight, easy to launch/land and non-hazardous in the event
107 of collision. The base cost is < \$75k and daily operating costs are primarily satellite data fees (\$25 to
108 \$55 typical). The vessel is 2 m in length, drafts 0.75 m, and weighs between 38 and 45 kg.
109 (depending on battery configuration). The boat has a fiberglass shell with a thick foam core
110 providing reserve buoyancy. The fin keel and rudder are designed to shed seaweed and debris and
111 have proven resistant to tangling in fishing lines and lobster and crab gear in previous missions. The
112 2 m tall mast has a bright orange sail for high visibility. A “Bermudan” style rig consists of a
113 reinforced carbon mast with high strength Dacron sails (main sail and a small jib) and chafe-resistant
114 lines. The *Nav2* is outfitted with an Airmar 200WX IPX7 marine grade meteorological sensor for
115 wind speed and direction for navigation/scientific purposes, as well as air temperature and barometric
116 pressure for scientific purposes. The *Nav2* is controlled via an iOS application (iPad or iPhone) that
117 is in constant communication to the boat using Wi-Fi, Cellular, or Iridium satellite in either manual
118 mode for line of sight control or autonomous mode for waypoint navigation (**Figure 2**), which
119 includes up-wind tacking in variable wind and sea states. A small electric thruster also provides back-
120 up propulsion for flat calm-wind conditions and for facilitating deployment and recovery, as needed.
121 The standard battery bank consists of up to 5 x LiFePO₄ batteries, for a total of 100 A hr and 1200 W
122 hr. Nominal 35 Watt solar panels provide solar recharge of the onboard battery bank for long
123 duration missions (up to several months).

124 A 3-channel fluorometer (Turner Designs Cyclops Integrator/C3) configured for measurement of
125 chlorophyll *a*, colored dissolved organic matter (CDOM; measured via fluorescence proxy), and

126 turbidity was installed in the hull, behind the main keel, facing downwards. In all cases, fluorometric
127 measurements are an imperfect measurement and are subject to artifacts. The chl. *a* and turbidity
128 channels underwent single-point cross-calibration using a natural estuarine sample in the laboratory,
129 referenced against a standard benchtop fluorometer that was recently calibrated. The CDOM channel
130 was calibrated instead using the same estuarine water sample, but filtered. The response from the
131 CDOM channel was calibrated using an associated absorption at 440 nm measured in a laboratory
132 spectrophotometer with a 10 cm path length.

133 3 Assessment

134 3.1 Vehicle performance

135 For the HAB monitoring trials, the *Nav2* vehicle was deployed from the beach three times between
136 Dec. 18, 2017 and Feb. 7, 2018, for deployments of increasing length of one, three, and seven days
137 (**Table 2; Figure 3**), in which case the boat traveled a total of 254 nautical miles (i.e. 470 km; 1 NM
138 = 1.9 km) at an average rate of 1.0 knots (1 knot = 1 NM hr⁻¹). Winds were relatively low during this
139 time period, corresponding to an overall average of 6.3 knots as compared to average monthly Dec.
140 and Jan. magnitudes of 10 to 13 knots¹.

141 Each mission was operated in a similar manner. The initial waypoints were entered in advance via
142 Wi-Fi using the chart-based app. Iridium satellite communication was used after deployment to
143 monitor the vehicles progress and send updated waypoints as desired, but all navigation was
144 controlled autonomously. To start each mission the *Nav2* was deployed from Sanibel Beach by hand
145 rolling the ASV on its cart out to a depth of > 0.75 m, pointing it offshore, and providing a mild push.
146 At the end of each mission the *Nav2* was directed to sail straight to shore until the keel grounded in
147 shallow water. The *Nav2* was then placed back onto the wheel cart and pulled on-shore. For the 25-
148 hour deployment beginning 2040 UTC Dec. 18, 2017 (**Figure 3a**), the *Nav2* was directed to head
149 straight out and back; sailing first nearly due south to a point 10 NM offshore and then returning
150 north to the beach. On the way back, in response to very calm winds, the thruster was turned on at
151 minimal power to provide a speed of 1 knot which was enough to reach shore at a convenient time
152 for pick up. Some drift was caused by local currents, which presents as a bend in the transect line.
153 Despite the boat experiencing a near full tidal cycle in both the southward and northward direction of
154 travel and experiencing winds between 0 and 3 knots for most of the deployment, the *Nav2* steadily
155 progressed. This first short mission served as a data collection test of the fluorometer, which was
156 logging to an SD card on board. For the 77-hour deployment beginning 1422 UTC Dec. 20, 2017
157 (**Figure 3b**), the *Nav2* was again deployed directly from Sanibel Beach. The intent of this mission
158 was to sail through an area with a known HABs bloom. The *Nav2* was directed to first travel south in
159 a zig-zag pattern to cover increased area compared to the first deployment. In response to updated
160 satellite imagery, the *Nav2* was then directed west 15 NM and then north returning to a convenient
161 pick up location at the NE limits of Sanibel Island. The decision was made to persist with sail power
162 for nearly the entire mission to better assess performance in the very calm wind conditions. Depending
163 on solar gain and battery status the thruster can be used for up to 48+ continuous hours to complete
164 straight transects in a timely manner. Tidal current drift effected the precision of transect lines when
165 the wind was < 3 knots. The vessel was removed from the water mid-deployment by a recreational
166 boater, who mistakenly assumed the vessel was lost, and who then traveled with the *Nav2* in a
167 northwest direction for 5 km. The *Nav2* was tracked during this time and contact was established
168 with the recreational boaters, who were instructed to place the vessel back into the water. At the end

¹ https://www.windfinder.com/windstatistics/southwest_of_tampa_bay_buoy

169 of this mission a more prominent statement was added to the Nav2's sail indicating boldly its nature
170 as a tracked and monitored research vessel. No such problem has occurred since. Near the end of the
171 mission the winds were calm and the thruster was used at low power to return in a timely manner for
172 pickup at the beach. For the 148-hour deployment beginning 1841 UTC Jan. 31, 2018 (**Figure 3c**),
173 the vessel was again deployed from Sanibel Beach with the intent of traversing a significant distance
174 of the West Florida Shelf. The vessel traveled west around Sanibel Island and then proceeded
175 northwards along the coast between 10 and 30 km offshore. After approaching Tampa Bay, the *Nav2*
176 was given waypoints to perform several longitudinal transects, until eventually being directed to the
177 south for retrieval at Venice Beach.

178 To evaluate the sailing capabilities of the *Nav2* vessel, a polar diagram was constructed (**Figure 4**).
179 The diagram illustrates the obtained vessel speed as a function of realized apparent winds as sensed
180 by the onboard wind sensor (**Figure 1**). For winds from angles directly behind the vessel to as far as
181 45° into the wind while under waypoint navigation, the vessel autonomously steers directly to the
182 desired destination and the colored lines represent Velocity Made good on Course (VMC). If the
183 *Nav2* is traveling towards a desired waypoint that happens to be directly into the wind (with a
184 threshold of 45° port or starboard), the vessel instead autonomously chooses to tack and achieves a
185 net Velocity Made Good (VMG) towards the waypoint. Represented in Figure 4 are therefore two
186 separate calculations; if winds are $< 45^\circ$ off of the bow, the VMG instead represents the apparent
187 velocity with respect to the destination. Increasing apparent wind velocities results in higher *Nav2*
188 velocities for speeds at least as high as 25 knots, under which conditions the vessel is capable of
189 traveling at average speeds > 2 knots. The *Nav2* is capable of reaching average speeds > 1 knot if
190 winds are at least 5 to 10 knots and greater than 60° away from the wind. Under low wind conditions
191 < 5 knots, the vessel realizes $VMC/VMG > 0.5$ knots for all apparent wind directions $> 30^\circ$. Overall,
192 the vessel is capable of realizing significant forward progress, regardless of wind direction, in all but
193 the most unfavorable wind conditions ($> 40 \text{ km day}^{-1}$).

194 To evaluate if there were effects of bubbles on the fluorometric data, the three measured parameters
195 were binned according to the wind speed at the time of data collection (**Figure 5**). We are assuming
196 in this case that higher wind speeds would generate more choppy ocean conditions and thus a larger
197 number of bubbles which may provide measurement artifacts both attenuating and amplifying
198 signals, depending on several factors. However, we observe that the fluorometric data does not
199 appear to depend on wind speed. While there is an increase in chl *a* values at lower apparent wind
200 speeds, this is likely just coincident with the *Nav2* experiencing lower winds closer to shore in the
201 first two deployments, in the presence of the confirmed algae bloom (described in the next section).

202 **3.2 Harmful algal bloom monitoring**

203 To determine if the *Nav2* is a viable platform for HAB detection and mapping, the chl. *a* data was
204 used as a proxy to provide information regarding algal densities. The same 3-channel fluorometer
205 was used as the primary detection means for chl. *a*. For the first two, shorter deployments, a large and
206 intense *K. brevis* (Florida Red Tide) bloom was present near shore ($\sim 2 \text{ km}$) towards which the vessel
207 was directed (**Figure 6a&b**). These deployments were intended to demonstrate the potential of the
208 *Nav2* for HAB mapping in localized areas in response to a bloom. The third deployment of 1-week
209 duration on the other hand was intended to demonstrate the potential for the boat to be used for
210 sustained, large-area HAB mapping, even in off-shore environments (**Figure 6c**). Generally, the
211 spatial trends of the in situ fluorometric data agreed well with the results from satellite imagery;
212 however, concentrations derived via remote sensing were significantly elevated compared to the in
213 situ data. For all three deployments, elevated chl. *a* south/southwest of Sanibel Island was probably

214 due primarily to *K. brevis*, given that this species was identified locally at cell counts exceeding
215 100,000 L⁻¹ (discrete samples in **Figure 6a-c**).

216 For the first deployment between Dec. 18 and 19, 2017 (**Figure 6a**), the vessel encountered an
217 elevated chl. *a* patch ~2.5 km south of the beach deployment location. Peak in situ concentrations in
218 the patch were ~ 6 µg L⁻¹ but were more typically between 1 and 3 µg L⁻¹. Interestingly, the initial
219 *Nav2* transect (i.e. southward) only recorded chl. *a* concentrations less than 1.5 µg L⁻¹, illustrating the
220 heterogeneity within the patch. In contrast, the remotely sensed background patch was larger and
221 concentrations were higher, between 5 and 50 µg L⁻¹. The second deployment between Dec. 20 and
222 23, 2017 again revealed a high degree of spatial heterogeneity. For the first portion of the deployment
223 chl. *a* concentrations rarely exceeded 2 µg L⁻¹. After traveling further west, the vessel soon
224 encountered two chl. *a* patches greater than 5 µg L⁻¹. Satellite data did not display a high matchup in
225 this case, as would be expected given that a 3-day composite was used; however, satellite data did
226 reveal that elevated chl. *a* was also observed with a patchy distribution. For the final deployment
227 beginning 5 weeks later between Jan. 31 and Feb. 6, 2018, in situ chl. *a* values were an order of
228 magnitude lower than in Dec. 2017. Just south of Sanibel Island, chl. *a* approached as high as 0.4 µg
229 L⁻¹, but then remained less than 0.2 µg L⁻¹ for most of the remainder of the deployment. The higher
230 values are consistent with the vessel being closer to shore, but also perhaps with a residual HAB
231 bloom, albeit *K. brevis* cell counts were below detection to the west of the deployment location.
232 While satellite chl. *a* was again much greater than the in situ *Nav2* data, its relative magnitude also
233 decreased by approximately an order of magnitude, with concentrations ~5 µg L⁻¹ nearshore and less
234 than 2 µg L⁻¹ for the offshore portion of the deployment. Interestingly, several portions of the color
235 track show conspicuously less chl. *a* despite little variations in other parameters, e.g. depth. Upon
236 further investigation, this phenomenon was revealed to be the result of diel variations (**Figure 7c**).
237 Very distinct depressions of the chl. *a* signal were observed between the daylight hours of 1300 and
238 2300 UTC (8:00 am and 6:00 pm locally). These variations are likely explainable by vertical diel
239 migration (Haphey-Wood, 1976) or by variations in pigment expression or measurement artifacts
240 (Babin et al., 1996). These intraday variations were not observed in other deployments where *K.*
241 *brevis* was likely present (or in the very first day of the 2018 deployment near confirmed *K. brevis*),
242 consistent with the knowledge that this organism does not migrate downwards during the day
243 (Schofield et al., 2006).

244 Turbidity and chl *a*. data provide further information regarding the environmental context of these
245 organisms (**Figure 8d-f**), as well as evidence for the proper functioning of the *Nav2*/fluorometer
246 package, i.e. that the data is consistent with expectations. The CDOM data is represented as
247 absorption at 440 nm despite being fluorometrically obtained. While this is not traditional, we argue
248 that an estimation of CDOM absorption is arguably more useful than representing data in more
249 traditional units (e.g. quinine-sulfate units), and a linear response would be expected either way.
250 Thus, while the CDOM magnitude may not be completely accurate (although values between 0.05
251 and 0.3 m⁻¹ are consistent with CDOM data measured at the Caloosahatchee River outflow)(Del
252 Castillo et al., 2000b)), the spatial variance in the observed CDOM should in fact be accurate. For all
253 three deployments, CDOM increased nearshore consistent with freshwater discharge from inlets,
254 both at deployment and retrieval sites but also during mid-deployment transects (e.g. Feb. 2, 2018;
255 **Figure 8f**). Other increases appear associated with *K. brevis* patches (based on the chl. *a* signature) or
256 river plumes (e.g. Dec. 19, 2017; **Figure 8d**). Along these lines, in the absence of a bloom and in a
257 coastline receiving discharge from a single freshwater source, the CDOM data may serve as a proxy
258 for salinity. Turbidity, being measured as the amount of light scattered at 90° from a source at a
259 single wavelength, appears to more reflect a combination of suspended sediment and phytoplankton

260 cells (**Figure 8g-i**). Turbidity measurements were more transient and less precise at a single location
261 than CDOM (e.g. Feb 3,4, 2018; **Figure 8i**), consistent with transient suspended sediments and a
262 heterogeneous water column. Winds were indeed in the 12 to 25 knot range Feb 3 from around UTC
263 0600 to 2200, and then periodically elevated on Feb. 4 throughout the day, which could provide an
264 explanation. Turbidity increases were also observed near *K. brevis* bloom patches (evidenced by
265 elevated chl. *a*; **Figure 8g**). It is notable that CDOM measurements have a higher precision than the
266 turbidity measurements (e.g. **Figure 8f&i**). This is expected because the dissolved CDOM will be
267 much more homogeneously mixed than will particulates measured via turbidity.

268 4 Discussion

269 4.1 Platform functionality

270 Though three deployments of increasing duration, the *Nav2* autonomous sail vehicle successfully
271 demonstrated the potential for the platform to provide mobile, unattended monitoring of the surface
272 coastal ocean. The *Nav2* is a unique platform in that it is small enough to be deployed in coastal and
273 inland waters, and by functioning identically to a real sailboat it can obtain high speeds and
274 accurately navigate and map areas of interest. The deployments demonstrated the vessel is robust
275 enough to reliably operate and survey under non-ideal sea states with winds up to 25 knots (although
276 we have tested the vehicle in winds > 30 knots in coastal waters of New England and Washington
277 State). Under conditions encountered in southwest Florida with winds averaging less than 4 knots,
278 however, the boat still managed to cover 17 to 22 NM per day, and 29 NM per day with winds
279 averaging 8 knots (**Table 2**). These winds were not necessarily directed from behind the boat; indeed,
280 the vessel can sail into the wind via autonomous tacking, under which significant forward progress is
281 still made at a VMG of 10 NM per day; **Figure 4**). The vessel is capable of efficiently reaching
282 preselected (or adjusted on the fly) waypoints (**Figures 2&3**). On the other hand, during deployment
283 and retrieval the boat can be operated manually in sailing mode, or with a thruster (**Table 2**). The
284 thruster is particularly useful in areas of high currents or ship traffic. Using the thruster only, the
285 *Nav2* can be used for short missions (up to 48 hours) without the sail.

286 We demonstrated deployments of up to one week. The vessel was operating exceptionally at the time
287 of retrieval and could have continued longer. Indeed, *Nav2* deployments since the time of writing this
288 report have lasted for 15+ days. Power efficiency improvements are ongoing with multi-sensor,
289 multi-month mission lengths feasible. Approximately 1 to 5 Watts extra power is available for
290 sensors. The power availability and length of mission will vary with solar conditions. In solar
291 conditions typical of Florida the panels typically provide an average of 200 W hrs day⁻¹. In low light
292 conditions typical of northern latitudes in the winter, mission planning needs to be adjusted
293 accordingly.

294 Deployment or retrieval of the *Nav2* is simple but exciting and can be achieved from a boat ramp or
295 from the beach under calm seas by a single operator. All three deployments described herein were
296 initiated from the beach. For deployment, the operator simply walks the small hand-held trailer into
297 the surf zone into waist-deep water until it is floating, and then slides the trailer out from underneath
298 the vessel. The operator can leave the iOS device on shore during the actual deployment or place it
299 into a waterproof case and hold with a lanyard. For retrieval the vehicle can be lifted back onto its
300 wheel cart by hand in shallow water and then pulled on shore. The *Nav2* is also capable of being
301 lifted from the water directly from a small boat. An easily overlooked aspect of using the vehicle is
302 the attention that it garners from beachgoers. This is an opportunity for community outreach, and the
303 southwest Florida HAB monitoring deployments were met with great inquiry and enthusiasm,

304 eventually becoming the subject of several media features. Unfortunately, however, this curiosity
305 also led to mission interruption on Dec. 22, 2017, when a recreational boater pulled the Nav2 from
306 the water and proceeded towards shore until seeing the contact information and statement on the
307 ASV. Under extremely low winds if the vessel is not obviously making forward progress it can
308 appear “lost”. Of course, theft is always an issue, especially of a smaller 2 m length boat. Future
309 versions of the vehicle are expected to be slightly larger to hold a larger number of sensors; this may
310 also serve the dual purpose of being a theft deterrent. The “curiosity” effect has been better managed
311 since these deployments by adding a large bold statement directly on the sail indicating the Nav2 is a
312 “RESEARCH VESSEL” “TRACKED AND MONITORED AT ALL TIMES”. Boaters are
313 increasingly aware that drones of all types on land or sea are carefully monitored. No problems with
314 curiosity or theft have occurred since. Other ongoing improvements with the *Nav2* vehicle include an
315 increased vehicle size to more easily accommodate a variety of sensors, the integration and testing of
316 additional sensors, refinements to the autonomous steering algorithm to reduce oversteering and
317 increase average speed, improved consistency of performing desirable straight data collection
318 transects in variable currents., and improved power efficiency to provide greater power for sensors
319 and in low light conditions.

320 4.2 Applications for Marine HAB monitoring.

321 The utility of the platform was demonstrated for the specific application of harmful algal bloom
322 monitoring of the Florida Red Tide species *Karenia brevis*. The recurring *K. brevis* blooms ravaging
323 southwest Florida are challenging to monitor because blooms are most detrimental nearshore, but in
324 many cases are transported shoreward from deeper waters ((Vargo, 2009)). While depth-resolved
325 measurements are ideal and have been routinely obtained by glider as part of the State of Florida
326 monitoring program, gliders have difficulty operating in waters less than 10 m deep, especially in
327 dynamic environments. Gliders are also more expensive to operate in shallow waters (they require
328 more frequent attention and battery and buoyancy pump servicing), prohibiting continuous operation.
329 Finally, gliders possess a limited selection of sensors and face many sensor design constraints,
330 currently limiting the wide-use of species-level detection techniques. Regardless, by the time *K.*
331 *brevis* blooms approach the coast, they are usually at the surface of a well-mixed water column and
332 the need for depth-resolved measurements is decreased (Robbins et al., 2006). Thus, there will for the
333 foreseeable future be a niche that must be filled for sustained coastal surface monitoring for this
334 species.

335 While the work presented herein only used a chl. *a* sensor (a common glider sensor), results serve as
336 justification for the investment into compatible HAB species-specific sensors. The fluorescence
337 response of organic matter has been extensively used as a proxy since terrestrially-based coastal
338 CDOM can, for discrete regions and time intervals, display nearly linear relationships with salinity
339 and FDOM (Coble, 1996; Del Castillo et al., 2000a). The success of the platform/sensor combination
340 is demonstrated by the matchup to satellite observations (**Figure 6**), repeatable diel variations
341 (**Figure 7**), obtainment of reasonable ancillary fluorometric data (**Figure 8**), and a lack of discernible
342 bubble artifacts (**Figure 5**). Interestingly, the chl. *a* data obtained in situ was of much lower
343 concentration than that detected by satellite. These variations can be expected based on the different
344 nature of the measurements. The fluorometric measurements of chl. *a* can be subject to various
345 packaging effects, especially at higher concentrations, and numerous accessory pigments can also
346 contribute to the signal (Babin et al., 1996; Schofield et al., 2006). Satellite measurements, on the
347 other hand, integrate over a depth interval and calculated concentrations are therefore representative
348 of an average concentration of the surface water column. They are also more challenging in turbid
349 and CDOM-rich optically complex waters where we conducted the deployments (Hu et al., 2005).

350 With a fleet of *Nav2* vehicles traveling ~20 NM per day in a repeatable triangular or “lawnmower”
351 raster pattern, several vehicles have the potential to continuously survey a large area, regardless of
352 water depth. The *Nav2* can also reveal more *K. brevis* surface heterogeneity than remote sensing data,
353 and data is acquired at a much greater temporal resolution. Therefore, the *Nav2*/fluorometer package
354 has the potential to provide satellite remote sensing ground-truthing data that can be used to improve
355 the species-specific algorithms. An unexpected result were the repeatable diel variations observed
356 during the longer mission (**Figure 7c**). Similar results have been observed in the same region of the
357 surface ocean during glider missions (unpublished). While not consistent with the behavior of *K.*
358 *brevis* cells, which instead exhibit positive phototaxis during the daylight hours (Schofield et al.,
359 2006), the resident phytoplankton appear to be either altering their surface expression of chl. *a* in an
360 excess of light or are descending to deeper waters, e.g. to obtain nutrients or alleviate photo stress
361 (Vargo, 2009). Overall, the high sensitivity and reproducibility of the measurements highlight the
362 functionality of the sensor for high precision measurements.

363 4.3 Other monitoring applications.

364 While chl. *a* measurements were the primary focus of this project, the ancillary fluorometric data
365 streams also shed light on some in water processes and allude to future applications of the *Nav2*
366 vessel. CDOM is of interest to biogeochemists for its role in dominating ocean color, playing a
367 critical role in photobiology, photochemistry (Helms et al., 2008), and photoproduction of CO₂
368 (Clark et al., 2004), contributing to aspects of the oceanic sulfur cycle (Gali et al., 2016), and
369 controlling the absorption of light energy and the subsequent impacts on heat flux (Hill, 2008) and
370 other ocean-climate interactions, and in serving as a tracer of freshwater (Fichot and Benner, 2012).
371 The fluorometrically measured CDOM exhibited intensities and spatial concentration distributions
372 that are expected in southwest Florida (Del Castillo et al., 2000a). Earlier in the project, we did install
373 a conductivity-temperature-depth CTD package onto the vehicle. However, conductivity
374 measurements were unreasonable, likely due to bubble retention in the flow cell. While we still aim
375 to resolve this issue with a different installation configuration, we can instead use CDOM as a rough
376 proxy for salinity, with the assumption that there is a single source of freshwater input that has a high
377 CDOM concentration (i.e. the Charlotte Harbor and the Caloosahatchee River).

378 The *Nav2* is inherently a meteorological sensor (e.g. for wind speed and magnitude, atmospheric
379 temperature, and humidity). Previously, the *Nav2* has been successfully configured with fisheries
380 sensors, including a pinger tracking hydrophone system (Sonotronics) and a cetacean and noise
381 monitoring hydrophone (Song Meter). Trials demonstrated successful location of crab tracking
382 pingers on the Washington coast and acoustic detection of various cetacean species. As of the time of
383 writing, we are currently adding a Wetlabs BB3 Scatterometer and a Solinst CT logger for HABs
384 surveys on Lake Okeechobee and the Indian River Lagoon in Florida. Addition of Oxygen/Temp
385 Optode (Aanderaa AADI) and CT sensors as well as an ADCP (Nortec) are under consideration to
386 provide a complete water quality monitoring suite.

387 5 Conclusions

388 The Navocean autonomous sail vehicle (*Nav2*) has been demonstrated to serve as a reliable mobile
389 platform for wide-area surface coastal monitoring. To our knowledge, this is the first demonstration
390 of a sail-driven vessel used for coastal HAB monitoring. The scientific results were shown to be
391 reasonable and have the potential to map HAB blooms and associated environmental conditions.
392 While the *Nav2* does not capture depth variations or collect instantaneous large surface area
393 measurements as do underwater gliders and satellites, respectively, the platform is a useful tool in the

394 arsenal for coastal or inland monitoring. The primary benefits of using the *Nav2* vehicle are that it is
395 fast and has reliable, autonomous navigation, has a completely renewable power source with no
396 consumables, can function in shallow or deep water inland or offshore, and is operable by a single
397 person. There are several additional demonstrated payload options as well as some currently in
398 preparation. At least with the planar-style optical sensors, bubbles do not appear to contribute
399 significant artifacts.

400 Harmful cyanobacterial blooms are increasing in intensity in global freshwater bodies (Paerl et al.,
401 2018). The *Nav2* vehicle is ideal for monitoring blooms in these frequently shallow lakes, especially
402 by limnologists who may have less training with more traditional oceanographic tools. To this end,
403 we are readying for deployments for freshwater *Microcystis aeruginosa* HAB monitoring in Lake
404 Okeechobee in the winter 2018-2019. Until the summer of 2018, there were few traditional
405 monitoring efforts, and no real-time water quality monitoring sensors on Lake Okeechobee, and even
406 now, only one stationary optical sensor is providing ground-truthing data for satellite efforts. We plan
407 to augment this fixed location monitoring with *Nav2* surveys to both add a mobile monitoring
408 element, but also to constrain the spatial variability of the surface optical properties in relation to
409 remote sensing data. A second 3-channel fluorometer is currently being installed to provide
410 phycoyanin and phycoerythrin measurements that help discriminate multiple algal species.
411 Eventually, we envision the *Nav2* platform as an essential part of multiple monitoring programs.

412 **6 Acknowledgements**

413 We would like to thank L. Kellie Dixon, Jim Hillier, and Karl Henderson at Mote, and last but not
414 least our former high school intern Gabriel Rey for assistance with field work.

415 **7 Conflict of Interest**

416 *The authors declare that the research was conducted in the absence of any commercial or financial*
417 *relationships that could be construed as a potential conflict of interest.*

418 **8 Author Contributions**

419 JB authored the manuscript, provided scientific oversight, and participated in field campaigns, EA is
420 the lead designer of the autonomous vehicle hardware and software, RC developed live data
421 visualization interface, EM coordinated field campaigns, and SD designed the sailboat and conducted
422 deployments.

423 **9 Funding**

424 This work was supported in part by a National Academies Gulf Research Program Early Career
425 Fellowship award #2000007281 that supporting salary and supplies, and the Gulf of Mexico Coastal
426 Ocean Observation System #NA16NOS0120018 that supported salaries.

427 **10 Data Availability Statement**

428 All datasets generated for this study are included in the manuscript and the supplementary files.

429 **11 References**

- 430 Anderson, D.M., Glibert, P.M. and Burkholder, J.M. (2002) Harmful algal blooms and
431 eutrophication: Nutrient sources, composition, and consequences. *Estuaries* 25, 704-726.
- 432 Babin, M., Morel, A. and Gentili, B. (1996) Remote sensing of sea surface Sun-induced chlorophyll
433 fluorescence: consequences of natural variations in the optical characteristics of phytoplankton and
434 the quantum yield of chlorophyll a fluorescence. *International Journal of Remote Sensing* 17, 2417-
435 2448.
- 436 Backer, L.C., McNeel, S.V., Barber, T., Kirkpatrick, B., Williams, C., Irvin, M., Zhou, Y., Johnson,
437 T.B., Nierenberg, K., Aabel, M., LePrell, R., Chapman, A., Foss, A., Corum, S., Hill, V.R., Kieszak,
438 S.M. and Cheng, Y.-S. (2010) Recreational exposure to microcystins during algal blooms in two
439 California lakes. *Toxicon* 55, 909-921.
- 440 Bowers, H. and Smith, G.J. (2017) Sensors for Monitoring of Harmful Algae, Cyanobacteria and
441 Their Toxins, in: Technologies, A.f.C. (Ed.), Workshop Proceedings. Moss Landing Marine
442 Laboratories, Moss Landing, CA.
- 443 Brand, L.E. and Compton, A. (2007) Long-term increase in *Karenia brevis* abundance along the
444 Southwest Florida Coast. *Harmful Algae* 6, 232-252.
- 445 Carmichael, W.W. (2001) Health Effects of Toxin-Producing Cyanobacteria: “The CyanoHABs”.
446 *Human and Ecological Risk Assessment: An International Journal* 7, 1393-1407.
- 447 Clark, C.D., Hiscock, W.T., Millero, F.J., Hitchcock, G., Brand, L., Miller, W.L., Ziolkowski, L.,
448 Chen, R.F. and Zika, R.G. (2004) CDOM distribution and CO₂ production on the southwest Florida
449 shelf. *Marine Chemistry* 89, 145-167.
- 450 Coble, P.G. (1996) Characterization of marine and terrestrial DOM in seawater using excitation
451 emission matrix spectroscopy. *Marine Chemistry* 51, 325-346.
- 452 Daniel, T., Manley, J. and Trenaman, N. (2011) The Wave Glider: enabling a new approach to
453 persistent ocean observation and research. *Ocean Dynamics* 61, 1509-1520.
- 454 Del Castillo, C.E., Gilbes, F., Coble, P.G. and Muller-Karger, F.E. (2000a) On the dispersal of
455 riverine colored dissolved organic matter over the West Florida Shelf. *Limnology and Oceanography*
456 45, 1425-1432.
- 457 Del Castillo, C.E., Gilbes, F., Coble, P.G. and Müller-Karger, F.E. (2000b) On the dispersal of
458 riverine colored dissolved organic matter over the West Florida Shelf. *Limnology and Oceanography*
459 45, 1425-1432.
- 460 Ducharme, J. (2018) Red Tide Is Killing Marine Life and Scaring Away Tourists in Florida. Here's
461 What to Know About It, *Time Magazine Online*.
- 462 Fichot, C.G. and Benner, R. (2012) The spectral slope coefficient of chromophoric dissolved organic
463 matter (S_{275–295}) as a tracer of terrigenous dissolved organic carbon in river-influenced ocean
464 margins. *Limnology and Oceanography* 57, 1453-1466.

- 465 Fleming, L.E., Rivero, C., Burns, J., Williams, C., Bean, J.A., Shea, K.A. and Stinn, J. (2002) Blue
466 green algal (cyanobacterial) toxins, surface drinking water, and liver cancer in Florida. *Harmful*
467 *Algae* 1, 157-168.
- 468 Gali, M., Kieber, D.J., Romera-Castillo, C., Kinsey, J.D., Devred, E., Perez, G.L., Westby, G.R.,
469 Marrase, C., Babin, M., Levasseur, M., Duarte, C.M., Agusti, S. and Simo, R. (2016) CDOM Sources
470 and Photobleaching Control Quantum Yields for Oceanic DMS Photolysis. *Environmental Science &*
471 *Technology* 50, 13361-13370.
- 472 Gannon, D.P., Berens McCabe, E.J., Camilleri, S.A., Gannon, J.G., Brueggen, M.K., Barleycorn,
473 A.A., Palubok, V.I., Kirkpatrick, G.J. and Wells, R.S. (2009) Effects of *Karenia brevis* harmful algal
474 blooms on nearshore fish communities in southwest Florida. *Marine Ecology Progress Series* 378,
475 171-186.
- 476 Happey-Wood, C.M. (1976) Vertical migration patterns in phytoplankton of mixed species
477 composition. *British Phycological Journal* 11, 355-369.
- 478 Helms, J.R., Stubbins, A., Ritchie, J.D., Minor, E.C., Kieber, D.J. and Mopper, K. (2008) Absorption
479 spectral slopes and slope ratios as indicators of molecular weight, source, and photobleaching of
480 chromophoric dissolved organic matter. *Limnology and Oceanography* 53, 955-969.
- 481 Hill, V.J. (2008) Impacts of chromophoric dissolved organic material on surface ocean heating in the
482 Chukchi Sea. *Journal of Geophysical Research-Oceans* 113, 10.
- 483 Hoagland, P., Jin, D., Polansky, L.Y., Kirkpatrick, B., Kirkpatrick, G., Fleming, L.E., Reich, A.,
484 Watkins, S.M., Ullmann, S.G. and Backer, L.C. (2009) The Costs of Respiratory Illnesses Arising
485 from Florida Gulf Coast *Karenia brevis* Blooms. *Environmental Health Perspectives* 117, 1239-1243.
- 486 Hu, C., Muller-Karger, F.E., Taylor, C., Carder, K.L., Kelble, C., Johns, E. and Heil, C.A. (2005)
487 Red tide detection and tracing using MODIS fluorescence data: A regional example in SW Florida
488 coastal waters. *Remote Sensing of Environment* 97, 311-321.
- 489 Kirkpatrick, B., Fleming, L.E., Backer, L.C., Bean, J.A., Tamer, R., Kirkpatrick, G., Kane, T.,
490 Wanner, A., Dalpra, D., Reich, A. and Baden, D.G. (2006) Environmental exposures to Florida red
491 tides: Effects on emergency room respiratory diagnoses admissions. *Harmful Algae* 5, 526-533.
- 492 McCabe, R.M., Hickey, B.M., Kudela, R.M., Lefebvre, K.A., Adams, N.G., Bill, B.D., Gulland,
493 F.M.D., Thomson, R.E., Cochlan, W.P. and Trainer, V.L. (2016) An unprecedented coastwide toxic
494 algal bloom linked to anomalous ocean conditions. *Geophysical Research Letters* 43, 10,366-
495 310,376.
- 496 Mordy, C.W., Cokelet, E.D., De Robertis, A., Jenkins, R., Kuhn, C.E., Lawrence-Slavas, N.,
497 Berchok, C.L., Crance, J.L., Sterling, J.T., Cross, J.N., Stabeno, P.J., Meinig, C., Tabisola, H.M.,
498 Burgess, W. and Wangen, I. (2017) *Advances in Ecosystem Research*
- 499 *Saildrone Surveys of Oceanography, Fish, and Marine Mammals in the Bering Sea. Oceanography*
500 30, 113-115.
- 501 O'Neil, J.M., Davis, T.W., Burford, M.A. and Gobler, C.J. (2012) The rise of harmful cyanobacteria
502 blooms: The potential roles of eutrophication and climate change. *Harmful Algae* 14, 313-334.

- 503 Paerl, H.W., Otten, T.G. and Kudela, R. (2018) Mitigating the Expansion of Harmful Algal Blooms
504 Across the Freshwater-to-Marine Continuum. *Environmental Science & Technology* 52, 5519-5529.
- 505 Reich, A., Lazensky, R., Faris, J., Fleming, L.E., Kirkpatrick, B., Watkins, S., Ullmann, S., Kohler,
506 K. and Hoagland, P. (2015) Assessing the impact of shellfish harvesting area closures on neurotoxic
507 shellfish poisoning (NSP) incidence during red tide (*Karenia brevis*) blooms. *Harmful Algae* 43, 13-
508 19.
- 509 Robbins, I.C., Kirkpatrick, G.J., Blackwell, S.M., Hillier, J., Knight, C.A. and Moline, M.A. (2006)
510 Improved monitoring of HABs using autonomous underwater vehicles (AUV). *Harmful Algae* 5,
511 749-761.
- 512 Schofield, O., Kerfoot, J., Mahoney, K., Moline, M., Oliver, M., Lohrenz, S. and Kirkpatrick, G.
513 (2006) Vertical migration of the toxic dinoflagellate *Karenia brevis* and the impact on ocean optical
514 properties. *Journal of Geophysical Research: Oceans* 111.
- 515 Scholin, C.A., Gulland, F., Doucette, G.J., Benson, S., Busman, M., Chavez, F.P., Cordaro, J.,
516 DeLong, R., De Vogelaere, A., Harvey, J., Haulena, M., Lefebvre, K., Lipscomb, T., Loscutoff, S.,
517 Lowenstine, L.J., Marin Iii, R., Miller, P.E., McLellan, W.A., Moeller, P.D.R., Powell, C.L., Rowles,
518 T., Silvagni, P., Silver, M., Spraker, T., Trainer, V. and Van Dolah, F.M. (2000) Mortality of sea
519 lions along the central California coast linked to a toxic diatom bloom. *Nature* 403, 80.
- 520 Shapiro, J., Dixon, L.K., Schofield, O.M., Kirkpatrick, B. and Kirkpatrick, G.J. (2015) Chapter 18 -
521 New Sensors for Ocean Observing: The Optical Phytoplankton Discriminator, in: Liu, Y., Kerkering,
522 H., Weisberg, R.H. (Eds.), *Coastal Ocean Observing Systems*. Academic Press, Boston, pp. 326-350.
- 523 Smith, D.R., King, K.W. and Williams, M.R. (2015) What is causing the harmful algal blooms in
524 Lake Erie? *Journal of Soil and Water Conservation* 70, 27A-29A.
- 525 Stockley, N.D., Sullivan, J.M., Hanisak, D. and McFarland, M.N. (2018) Using observation networks
526 to examine the impact of Lake Okeechobee discharges on the St. Lucie Estuary, Florida, SPIE
527 Defense + Security. SPIE, p. 8.
- 528 Vargo, G.A. (2009) A brief summary of the physiology and ecology of *Karenia brevis* Davis (G.
529 Hansen and Moestrup comb. nov.) red tides on the West Florida Shelf and of hypotheses posed for
530 their initiation, growth, maintenance, and termination. *Harmful Algae* 8, 573-584.
- 531

532 Table 1 – Specifications for the *Nav2* Autonomous Sail Vehicle (Navocean).

Nav2 ASV Specifications and Capabilities	
Mission Duration	Up to 6 months
Speed	1-3 Knots
Length	2m (6.5')
Draft	.75m (2.5')
Weight	85 lbs plus payload
Rigging	Main + Jib "storm" sails and chafe resistant lines
Mast	Unstayed reinforced carbon
Winch	Electric with anti-jamming spool
Rudder and Keel	No-tangle design sheds lines and seaweed
Power	12 Volt, 35 W solar array
Batteries	Up to 120 Ah LiFePO4
Standard Sensors	GPS, PRH, Meteorological, AIS
Optional Sensors	Water Quality: O ₂ , CT, backscatter, 3/6 channel fluorometer (chl. a, phycocyanin, phycoerythrin, CDOM, turbidity, oil) Acoustic: Pinger Tracking, Cetaceans, Telemetry Custom: ADCP and many others
Navigation	Autonomous to waypoints + manual option
Charts	NOAA RNC included
UI	Chart based iOS App + web portal
Dashboard	Location, speed, course, heading, true and apparent wind, pitch, roll, power, battery and solar voltage, sail and rudder position, thruster RPM, connectivity status, waypoint ETA
Comms	Iridium SBD (Sat), Cell, and WiFi
Real-time	Configurable telemetry and sensor data

533

534

535

536

Autonomous Sail-Powered Surface Vehicle Harmful Algal Bloom Monitoring

537 Table 2 – Summary of the environmental conditions and the *Nav2* ASV performance during harmful
538 algae bloom tracking deployments. The distance covered includes periods of using the thruster at low
539 speeds (~ 1 knot) in calm winds to return the ASV to shore for a convenient pickup time.
540 Alternatively, the thruster can be used temporarily to complete important transects if the wind dies or
541 for entire short missions of ~ 1 day.

MISSION DATES	NUMBER OF HOURS	WIND SPEED AVERAGE (Apparent)	BOAT SPEED AVERAGE (Knots)	SEA STATE BEAUFORT (Range)	DISTANCE COVERED (NM)	Percent Thruster Use
Dec 18 to 19, 2017	25	3.2	0.9	0-2	22.5	12%
Dec 21 to 24, 2017	77	3.6	0.7	0-3	53.9	10%
Jan 31 to Feb 06, 2018	148	8.2	1.2	0-5	177.6	3%

542

In review

543 **Figure Captions**

544 Figure 1 – Diagram of the Navocean Nav2 Autonomous Sail Vehicle and components.

545 Figure 2 – Screenshots of the iOS control software running on an iPad, illustrating operation via
546 Manual Control (A) or via Waypoint navigation (B).

547 Figure 3 – Screenshots of the iOS control software running on an iPad, illustrating the three ASV
548 tracks in southwest Florida for the purposes of harmful algal bloom monitoring from deployments
549 between (A) Dec. 18 and 19, 2017, (B) Dec. 20 and 23, 2017, and (C) Jan. 31 and Feb. 6, 2018.
550 Waypoints

551 Figure 4 – A polar diagram illustrating averaged *Nav2* velocity magnitude while sailing as a function
552 of apparent wind magnitude and direction for all deployments. The four colors represent data for
553 intervals for binned wind speeds. Between angles of 45° and 180°, the magnitude is the actual
554 realized velocity over ground of the vehicle in the intended direction, or the “Velocity Made Good on
555 Course”. The *Nav2* tacks as does a traditional sailboat at wind angles < 45°, realizing VMG
556 (“Velocity Made Good”), and the vessel makes significant forward progress even when traveling at
557 very low angles relative to the wind.

558 Figure 5 – For all deployments, the fluorometer data were binned by their associated 5-knot interval
559 apparent winds speeds to determine if wind and associated bubbles exhibited an artifact.

560 Figure 6 – *Chl. a* colormaps or colortracks are presented as demonstrating of HAB mapping
561 capabilities from the three *Nav2* deployments. Background MODIS satellite image is courtesy of Dr.
562 Chuanmin Hu at University of South Florida, and the *K. brevis* cell count data was collected as part
563 of the Florida Fish and Wildlife Commission / Mote Marine Red Tide Monitoring Partnership. The
564 single return raster leg from the deployment during Dec. 18 to 19, 2017 warrants data representation
565 as an interpolated colormap (between 0 and 4 $\mu\text{g L}^{-1}$) with an overlain boat track (black line), (A); A
566 colortrack is used to represent (B) the Dec. 20-23, 2017 data (between 0 and 4 $\mu\text{g L}^{-1}$), and (C) the
567 Jan. 31 – Feb. 6, 2018 data (between 0 and 0.4 $\mu\text{g L}^{-1}$). The background MODIS images are 1-, 3-,
568 and 7-day composites, respectively, and the colors in all represent between 0 and 60 $\mu\text{g L}^{-1}$ remotely-
569 sensed *chl. a* (Note: gray colors indicate areas with cloud cover and no data). Discrete samples
570 collected and enumerated for *K. brevis* cells within 1 week of the deployments are represented by
571 circular icons: grey indicates not present/background levels, white indicates very low densities
572 >1,000-10,000 cells L^{-1} , yellow indicates low densities 10,000 – 100,000 cells L^{-1} , orange indicates
573 medium densities 100,000 – 1,000,000 cells L^{-1} , and red indicates high > 1,000,000 cells L^{-1} .

574 Figure 7 –To examine diel trends, daily time series for *chl. a* are presented for the (A) Dec. 18-19,
575 2017, (B) Dec. 20-23, 2017, and (C) Jan. 31 – Feb. 6, 2018 deployments. Multiple days are depicted
576 on the same plots. Note, the y-axis magnitudes are different for the Jan. 31 to Feb. 6, 2018
577 deployment.

578 Figure 8 – For the Dec. 18 to 19, 2017, Dec. 20 to 23, 2017, and Jan. 31 to Feb. 6, 2018 deployments,
579 the *chl. a* time series is represented in (A) – (C) respectively, CDOM measured via fluorometric
580 proxy is represented in (D) – (F) (explanation in text), and turbidity is represented in (G) – (I). Note,
581 the y-axis magnitudes are different for the Jan. 31 to Feb. 6, 2018 deployment.

Figure 1.JPEG

bioRxiv preprint doi: <https://doi.org/10.1101/473827>; this version posted November 19, 2018. The copyright holder for this preprint (which was not certified by peer review) is the author/funder, who has granted bioRxiv a license to display the preprint in perpetuity. It is made available under aCC-BY-NC-ND 4.0 International license.

Figure 1

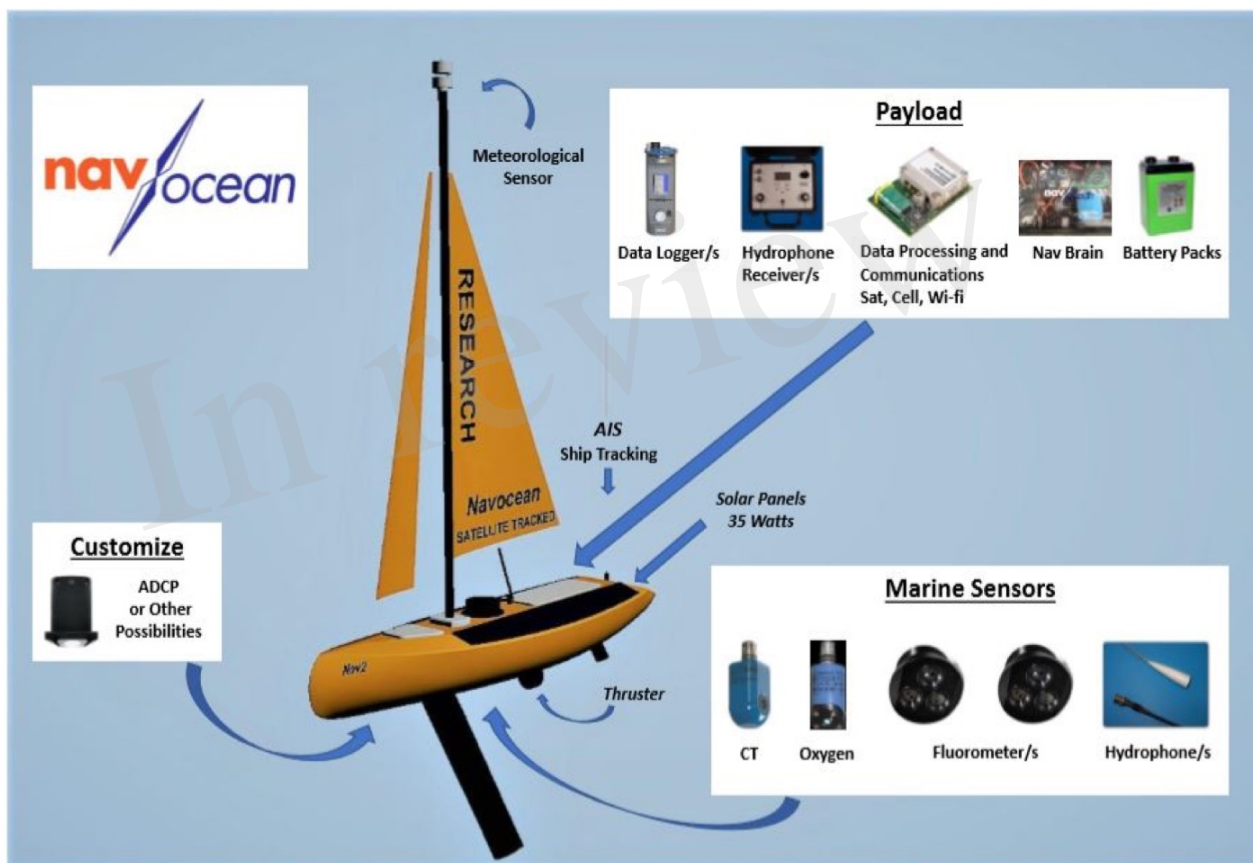


Figure 2.JPEG

bioRxiv preprint doi: <https://doi.org/10.1101/473827>; this version posted November 19, 2018. The copyright holder for this preprint (which was not certified by peer review) is the author/funder, who has granted bioRxiv a license to display the preprint in perpetuity. It is made available under aCC-BY-NC-ND 4.0 International license.

Figure 2

a)



b)

The 'NEW ACTION' screen includes the following options and fields:

- Waypoint**: Lat [] °, Lon [] °, rad 400 m, (optional name) ABCDEF, tack cor 30... m
- Set Course**: [] °
- Point Upwind**
- Full Stop**
- Start Over at #**: 1, repeat 7 times

Figure 3.JPEG

bioRxiv preprint doi: <https://doi.org/10.1101/473827>; this version posted November 19, 2018. The copyright holder for this preprint (which was not certified by peer review) is the author/funder, who has granted bioRxiv a license to display the preprint in perpetuity. It is made available under aCC-BY-NC-ND 4.0 International license.

Figure 3

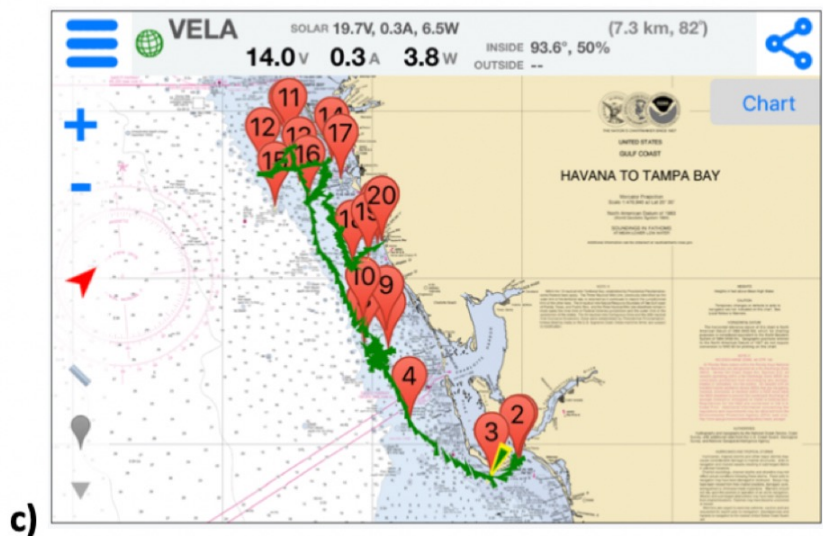
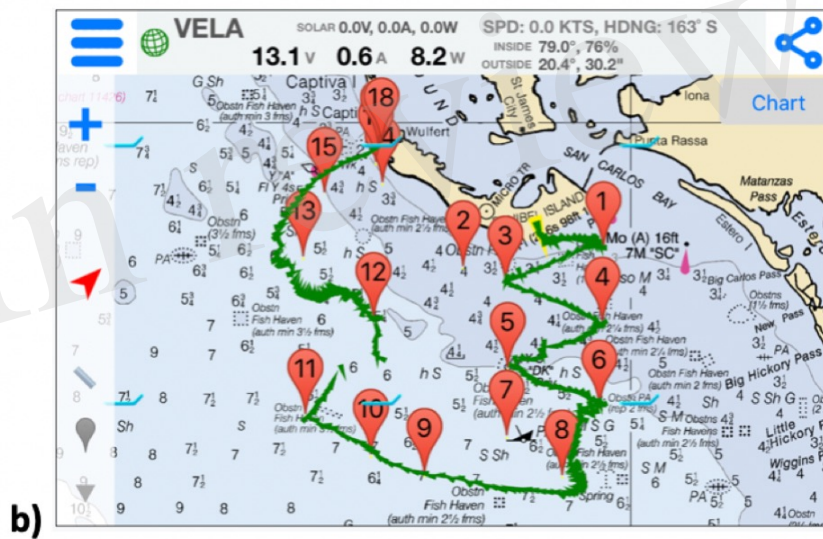
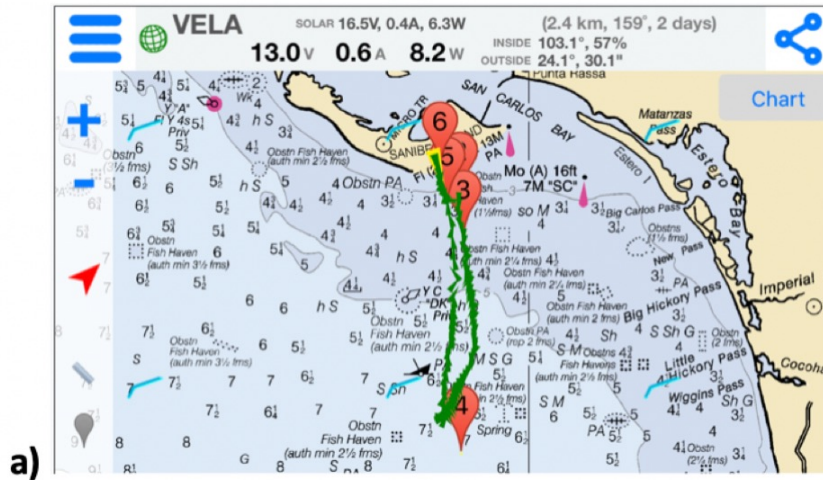


Figure 4.JPEG

bioRxiv preprint doi: <https://doi.org/10.1101/473827>; this version posted November 19, 2018. The copyright holder for this preprint (which was not certified by peer review) is the author/funder, who has granted bioRxiv a license to display the preprint in perpetuity. It is made available under aCC-BY-NC-ND 4.0 International license.

Figure 4

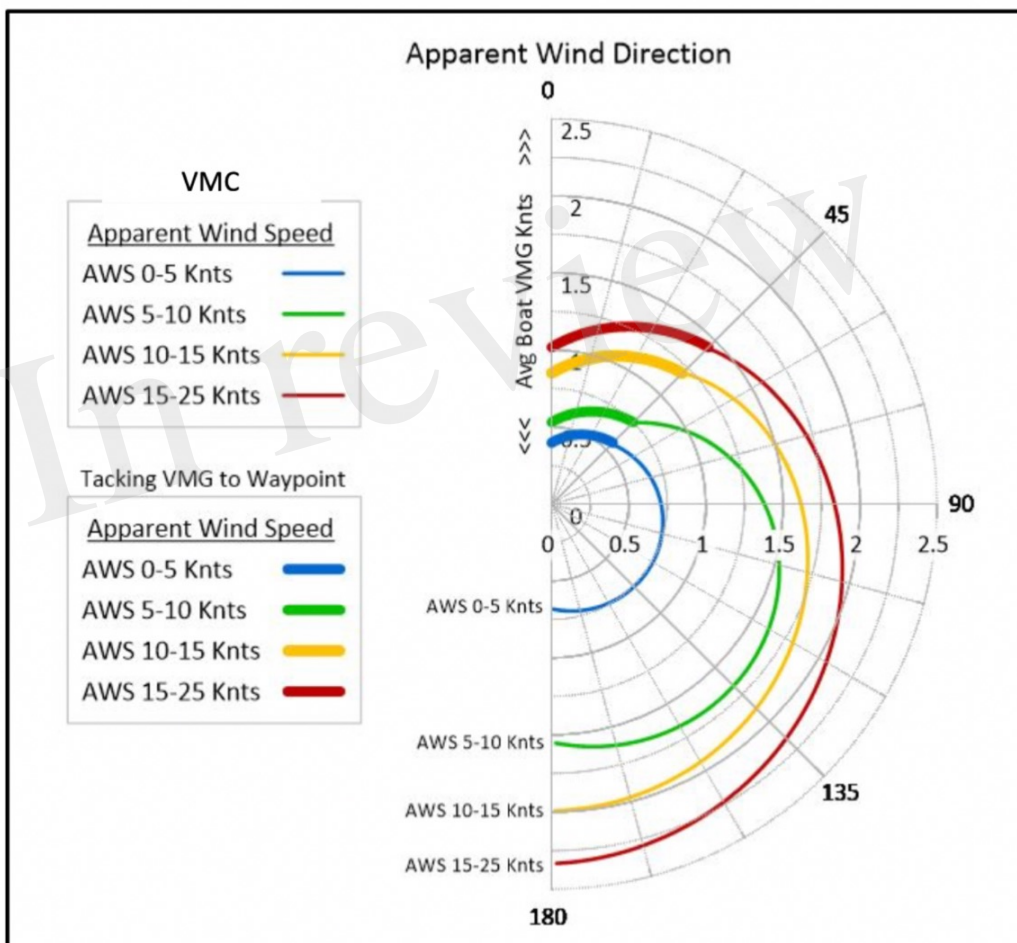


Figure 5.JPEG

bioRxiv preprint doi: <https://doi.org/10.1101/473827>; this version posted November 19, 2018. The copyright holder for this preprint (which was not certified by peer review) is the author/funder, who has granted bioRxiv a license to display the preprint in perpetuity. It is made available under aCC-BY-NC-ND 4.0 International license.

Figure 5

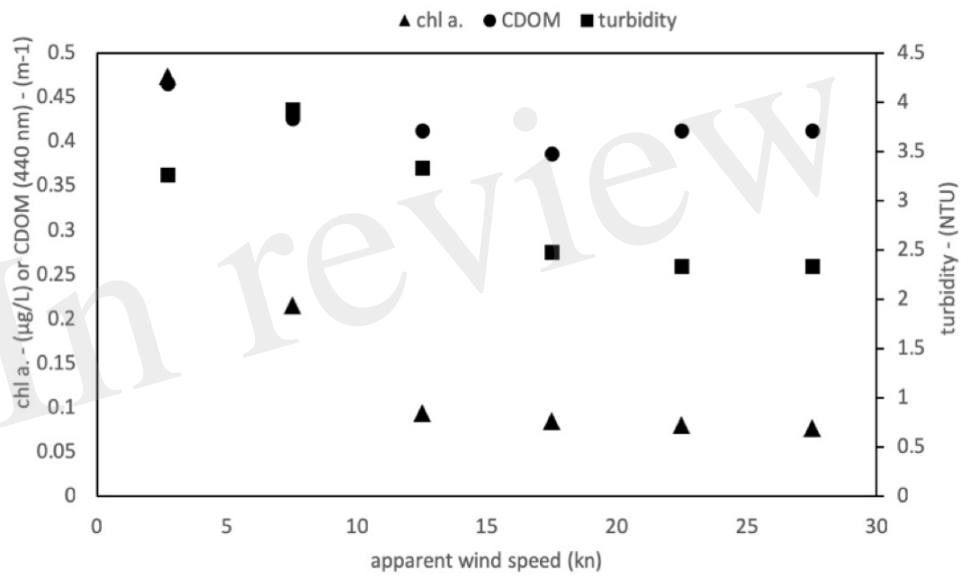
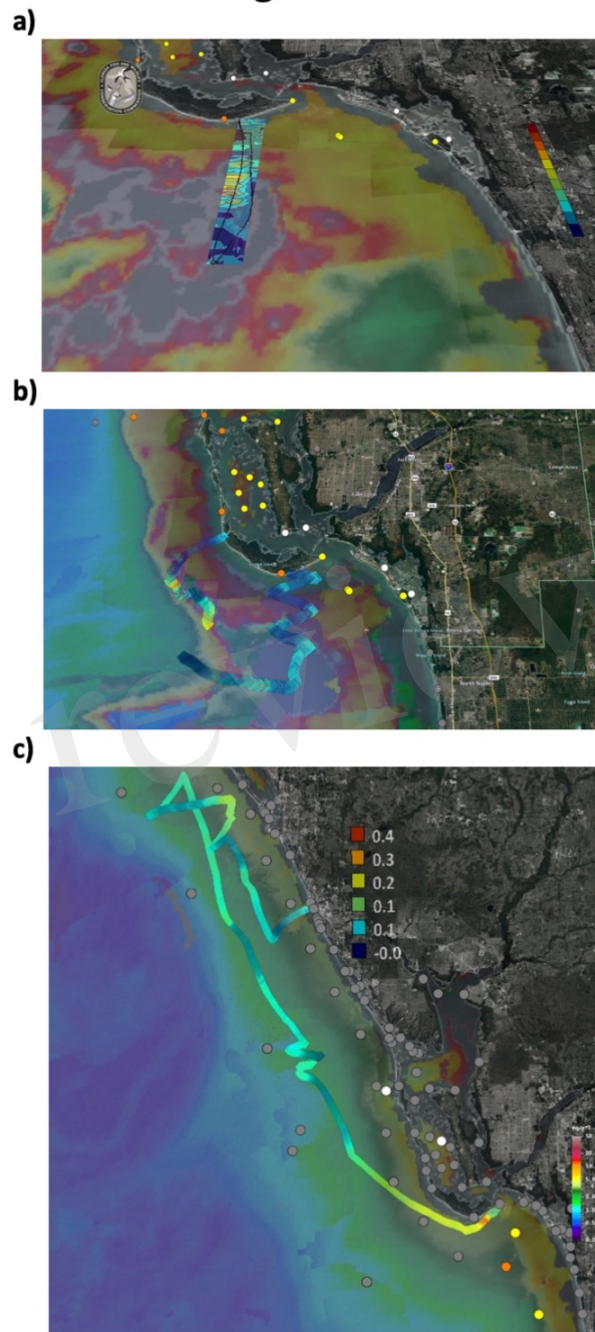


Figure 6.JPEG

bioRxiv preprint doi: <https://doi.org/10.1101/473827>; this version posted November 19, 2018. The copyright holder for this preprint (which was not certified by peer review) is the author/funder, who has granted bioRxiv a license to display the preprint in perpetuity. It is made available under aCC-BY-NC-ND 4.0 International license.

Figure 6



bioRxiv preprint doi: <https://doi.org/10.1101/473827>; this version posted November 19, 2018. The copyright holder for this preprint (which was not certified by peer review) is the author/funder, who has granted bioRxiv a license to display the preprint in perpetuity. It is made available under aCC-BY-NC-ND 4.0 International license.

Figure 7

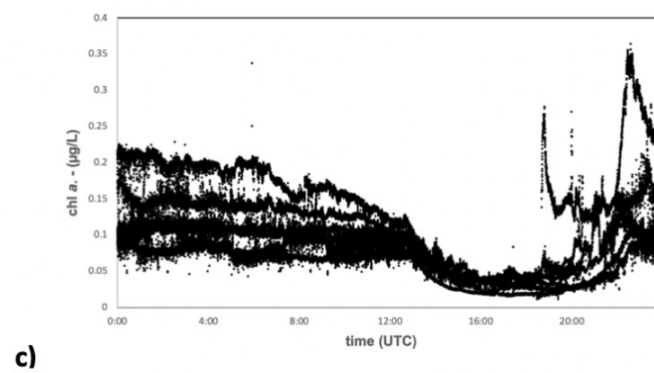
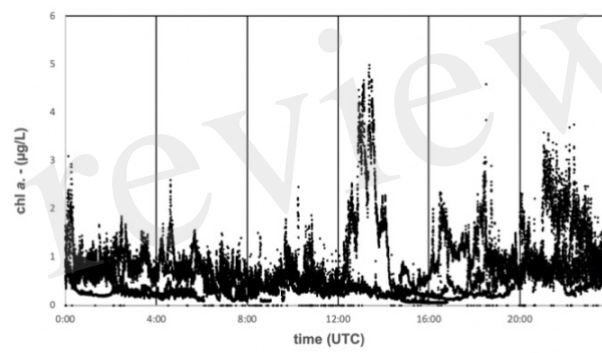
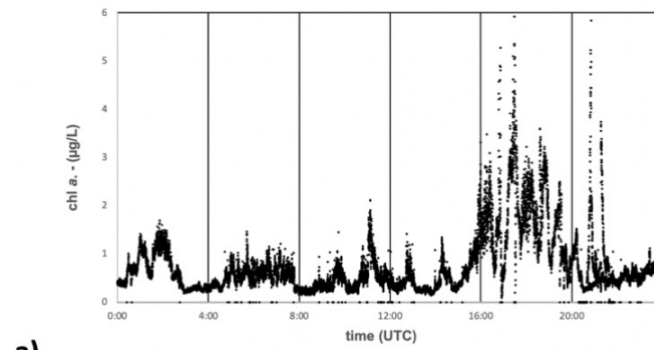


Figure 8.JPEG

bioRxiv preprint doi: <https://doi.org/10.1101/473827>; this version posted November 19, 2018. The copyright holder for this preprint (which was not certified by peer review) is the author/funder, who has granted bioRxiv a license to display the preprint in perpetuity. It is made available under aCC-BY-NC-ND 4.0 International license.

Figure 8

